

Molecular evaluation of herbal compounds as potent inhibitors of acetylcholinesterase for the treatment of Alzheimer's disease

YAN-XIU CHEN¹, GUAN-ZENG LI¹, BIN ZHANG², ZHANG-YONG XIA¹ and MEI ZHANG³

¹Department of Neurology, Liaocheng People's Hospital and Liaocheng Clinical School of Taishan Medical University;

²Department of Neurology, The 3rd People's Hospital of Liaocheng, Liaocheng, Shandong 252000;

³Department of Neurology, The 5th People's Hospital of Wuhan, Wuhan, Hubei 430050, P.R. China

Received June 15, 2015; Accepted April 15, 2016

DOI: 10.3892/mmr.2016.5244

Abstract. Alzheimer's disease (AD) is a progressive disease and the predominant cause of dementia. Common symptoms include short-term memory loss, and confusion with time and place. Individuals with AD depend on their caregivers for assistance, and may pose a burden to them. The acetylcholinesterase (AChE) enzyme is a key target in AD and inhibition of this enzyme may be a promising strategy in the drug discovery process. In the present study, an inhibitory assay was carried out against AChE using total alkaloidal plants and herbal extracts commonly available in vegetable markets. Subsequently, molecular docking simulation analyses of the bioactive compounds present in the plants were conducted, as well as a protein-ligand interaction analysis. The stability of the docked protein-ligand complex was assessed by 20 ns molecular dynamics simulation. The inhibitory assay demonstrated that *Uncaria rhynchophylla* and *Portulaca oleracea* were able to inhibit AChE. In addition, molecular docking simulation analyses indicated that catechin present in *Uncaria rhynchophylla*, and dopamine and norepinephrine present in *Portulaca oleracea*, had the best docking scores and interaction energy. In conclusion, catechin in *Uncaria rhynchophylla*, and dopamine and norepinephrine in *Portulaca oleracea* may be used to treat AD.

Introduction

Alzheimer's disease (AD) is a chronic neurodegenerative disease, which accounts for the majority of dementia cases (1). Common symptoms of AD include short-term memory loss, disorientation, loss of motivation, mood swings and behavioral issues (1,2). Patients with AD often withdraw from family and society as their condition declines (3,4).

The cause of AD is not fully understood (1), and researchers have hypothesized that ~70% of the risk is due to genetic factors (4), followed by other factors, including head injuries, depression or hypertension (4-7). Patients with AD rely on caregivers for assistance, and in certain cases they may pose a burden to them (6). In developed countries, AD is considered to be one of the most financially challenging diseases (8-11). The underlying mechanisms of AD are not fully known and the majority of available drug therapies are based on the cholinergic hypothesis (12). The cholinergic hypothesis proposes that AD results from reduced synthesis of the neurotransmitter acetylcholine (ACh) (12). Houghton *et al* (13) indicated that inhibiting the enzyme acetylcholinesterase (AChE), which breaks down ACh, is a promising strategy for treating patients with AD. There are alternative hypotheses, such as the amyloid (14) and tau (15) hypotheses; however, AChE is a favorable enzyme target for numerous researchers. Furthermore, AChE has garnered more attention regarding its screening potential, and the identification of AChE novel inhibitors from various natural products, including plants and herbal extracts.

The enzyme AChE is a hydrolase of the carboxylesterase family, which hydrolyzes the neurotransmitter ACh (16,17). It is primarily present in the neuromuscular junctions and cholinergic brain synapses, assisting in the termination of synaptic transmissions. It belongs to the carboxylesterase family of enzymes (18,19). During neurotransmission, ACh is released from the nerve into the synaptic cleft where it binds to ACh receptors on the post-synaptic membrane, relaying the signal from the nerve (20). AChE is located on the post-synaptic membrane and terminates the signal transmission by hydrolyzing ACh (21). The liberated choline is then taken up by the pre-synaptic nerve and ACh is synthesized by combining with acetyl-CoA through the action of choline acetyltransferase (22).

The present study performed an inhibitory assay to determine the inhibitory activity of certain plant extracts against human AChE. In addition, computational research employing virtual screening of the compounds present in the plant extracts and AChE retrieved from the Protein Data Bank (PDB ID: 4PQE) was conducted, using the molecular docking simulation protocol. Subsequently, a protein-ligand interaction analysis was performed with 20 ns molecular dynamics (MD) simulation.

Correspondence to: Dr Mei Zhang, Department of Neurology, The 5th People's Hospital of Wuhan, 122 Xianzheng Street, Wuhan, Hubei 430050, P.R. China
E-mail: meizhang918@gmail.com

Key words: Alzheimer's disease, acetylcholinesterase, molecular docking, molecular dynamics

Table I. Inhibitory activity of the total alkaloidal extracts (100 µg/ml final concentration) against AChE.

| SN | Scientific name | Parts used | Yield | AChE inhibition (%) |
|----|------------------------------|-------------|-------|---------------------|
| 1 | <i>Allium sativum</i> | Bulb | 0.44 | 33.8 |
| 2 | <i>Areca catechu</i> | Fruit | 0.66 | 19.3 |
| 3 | <i>Camellia sinensis</i> | Leaves | 0.51 | 40.2 |
| 4 | <i>Curcuma longa</i> | Root | 0.27 | 35.8 |
| 5 | <i>Lobelia chinensis</i> | Whole plant | 0.21 | 28.2 |
| 6 | <i>Nelumbo nucifera</i> | Leaves | 0.34 | 76.5 |
| 7 | <i>Portulaca oleracea</i> | Stem | 0.24 | 74.2 |
| 8 | <i>Uncaria rhynchophylla</i> | Stem | 0.41 | 78.4 |
| 9 | <i>Zingiber officinale</i> | Root | 0.43 | 60.5 |

AChE, acetylcholinesterase; SN, serial number.

Table II. Compounds associated with the herbal plants and their NCBI Pubchem ID.

| SN | Plant | Chemical composition | Pubchem ID |
|----|------------------------------|----------------------|-------------|
| 1 | <i>Nelumbo nucifera</i> | Miquelianin | CID 5274585 |
| | | Coclaurine | CID 160487 |
| | | Higenamine | CID 114840 |
| | | Nuciferine | CID 3108374 |
| 2 | <i>Portulaca oleracea</i> | Norepinephrine | CID 439260 |
| | | Dopamine | CID 681 |
| | | L-DOPA | CID 6047 |
| 3 | <i>Uncaria rhynchophylla</i> | Catechin | CID 9064 |
| | | Rhynchophylline | CID 3033948 |
| 4 | <i>Areca catechu</i> | Arecaidine | CID 10355 |
| | | Arecoline | CID 2230 |
| 5 | <i>Lobelia chinensis</i> | Lobeline | CID 101616 |
| | | Lobelanine | CID 442647 |
| | | Lobelanidine | CID 96946 |
| 6 | <i>Curcuma longa</i> | Curcumin | CID 969516 |
| 7 | <i>Zingiber officinale</i> | Zingerone | CID 31211 |
| | | Shogaol | CID 5281794 |
| | | Gingerol | CID 442793 |
| 8 | <i>Allium sativum</i> | Allicin | CID 65036 |
| | | Ajoene | CID 5386591 |
| 9 | <i>Camellia sinensis</i> | Gallocatechol | CID 65084 |

NCBI, National Center for Biotechnology Information; SN, serial number; L-DOPA, L-3,4-dihydroxyphenylalanine.

Materials and methods

AChE inhibitory assay. The following plant samples with medicinal properties were collected: *Allium sativum*, *Areca catechu*, *Camellia sinensis*, *Curcuma longa*, *Lobelia chinensis*, *Nelumbo nucifera*, *Portulaca oleracea*, *Uncaria rhynchophylla* and *Zingiber officinale*. The majority of the collected samples are commonly available in vegetable and herbal medicine markets. Approximately 120 g of each of the plant samples was crushed to a powder using a pestle

and mortar. Each of the samples was then treated with 95% ethanol and was refluxed for 2 h to collect the alcohol extract. The extract was further evaporated, air-dried and suspended in deionized water. The pH of the suspension was adjusted to 2.0. The aqueous solution from the alkaloidal extracts, which is acidic in nature, was filtered following an overnight incubation, the pH was adjusted to 10.0 and the extract was obtained using chloroform. The layers of chloroform were evaporated and air dried. The final alkaloidal extracts obtained were used to conduct the AChE inhibitory assay, which was purchased from

Table III. Molecular docking scores of the compounds.

| Ligand | Source | Rerank score | MolDock score | Interaction | HBond |
|-------------|------------------------------|--------------|---------------|-------------|--------|
| CID 9064 | <i>Uncaria rhynchophylla</i> | -67.43 | -91.57 | -114.847 | -11.47 |
| CID 681 | <i>Portulaca oleracea</i> | -64.76 | -84.07 | -86.940 | -12.38 |
| CID 439260 | <i>Portulaca oleracea</i> | -60.40 | -81.88 | -83.460 | -12.14 |
| CID 31211 | <i>Zingiber officinale</i> | -59.39 | -46.98 | -48.230 | -3.87 |
| CID 65084 | <i>Camellia sinensis</i> | -53.40 | -71.24 | -78.860 | -9.88 |
| CID 6047 | <i>Portulaca oleracea</i> | -50.14 | -36.84 | -32.170 | -9.71 |
| CID 65036 | <i>Allium sativum</i> | -49.10 | -29.47 | -26.750 | -2.02 |
| CID 442793 | <i>Zingiber officinale</i> | -48.79 | -72.86 | -73.050 | -2.16 |
| CID 114840 | <i>Nelumbo nucifera</i> | -45.15 | -47.37 | -55.850 | -8.94 |
| CID 160487 | <i>Nelumbo nucifera</i> | -43.02 | -51.27 | -59.170 | -5.89 |
| CID 5386591 | <i>Allium sativum</i> | -40.22 | -10.84 | -6.720 | -1.65 |
| CID 5281794 | <i>Zingiber officinale</i> | -39.29 | -73.70 | -67.630 | -7.49 |

MolDock, molecular docking; HBond, hydrogen bond.

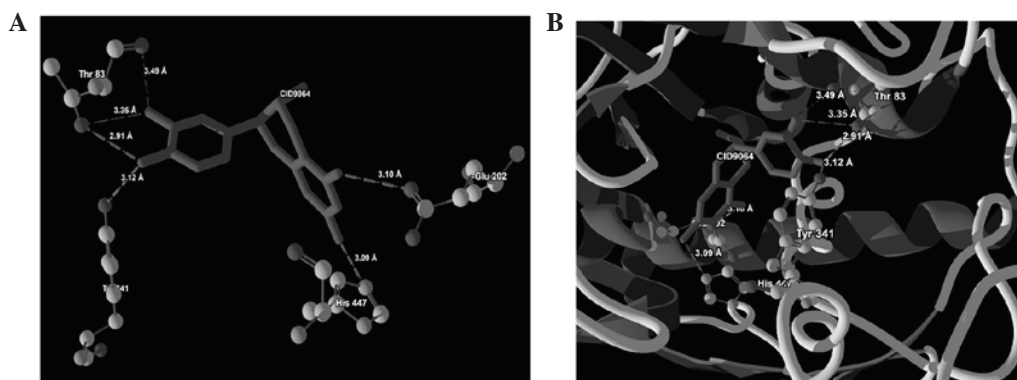


Figure 1. (A) Binding mode of CID9064 at the active site region of AChE. (B) Secondary structure depicting the strong molecular interactions formed between CID681 and Thr83, Glu202, Thr341 and His447 residues of AChE. AChE, acetylcholinesterase.

Sigma-Aldrich (St. Louis, MO, USA). The AChE inhibitory assay was performed according to the protocol developed by Ellman *et al* (23) with slight modifications. Briefly, a mixture containing 100 μ l 0.1M NaH_2PO_4 (pH 8.0), 25 μ l plant extract solution (1 mg/ml) and 20 μ l AChE enzyme (0.20 U/ml) was incubated for 30 min at 4°C. Subsequently, ~15 μ l 0.01 M 5,5'-dithiobis(2-nitrobenzoic acid) mixed with 10 μ l 0.05 M acetylthiocholine iodide was incubated with the mixture at 37°C for 30 min. The optical density of the final solution was measured at 405 nm (ELC800 Absorbance Microplate Reader; BioTek Instruments, Inc., Winooski, VT, USA), and enzyme activity was calculated by comparing the reaction rate of the samples relative to a blank solution. The percentage of inhibitory activity was calculated by subtracting the enzyme activity percentage from 100%.

Molecular docking. The molecular docking simulation was performed using the Molegro Virtual Docker 5.0 (CLC Bio, Aarhus, Denmark). Briefly, the 2D structures of the compounds present in the plant samples were retrieved from the National Center for Biotechnology Information (NCBI) PubChem database (<https://pubchem.ncbi.nlm.nih.gov>). Their geometries

were optimized using the MM2 force field and were converted to a 3D format (sybyl mol2 file format). AChE retrieved from the PDB (ID: 4PQE) was then loaded into the Molegro Virtual Docker. The bind site was set having a sphere of 15 Å radius and the following coordinates: X, -27.90; Y, 22.91; Z, -10.18.

For the molecular docking simulation, the bonds of all the compounds were set flexible, and for the protein the residues in the binding site were set flexible with a tolerance of 1.0 and strength of 0.80. The side chain and torsional degrees of freedom for the flexible residues and ligands were subjected to 2,000 steps of energy minimization. Flexible molecular docking simulations were performed setting the MolDock Grid scoring function (24) with a grid resolution of 0.30 Å. The search algorithm was set for MolDock SE with 20 runs for each compound, with a maximum of 1,500 iterations and population size of 50. The in-depth molecular interaction was inspected using a ligand energy inspector. The ligand energy inspector evaluates the energy interactions for a given docked ligand with the interacting amino acids. In the present study, the in-depth molecular interaction was inspected using a ligand energy inspector. The ligand energy inspector evaluates the energy interactions for a given docked ligand with the interacting amino acids.

Table IV. Molecular interaction analysis of the top hits.

| SN | Ligand | Protein-ligand | Interaction energy (kJ/mol) | Interaction distance (Å) |
|----|-----------|------------------|-----------------------------|--------------------------|
| 1 | CID9064 | Thr83(OG1)-O(5) | -2.50 | 2.91 |
| | | Thr83(OG1)-O(4) | -1.26 | 3.35 |
| | | Thr83(O)-O(4) | -0.55 | 3.49 |
| | | Thr341(OH)-O(5) | -2.40 | 3.12 |
| | | His447(NE2)-O(3) | -2.50 | 3.09 |
| | | Glu202(OE1)-O(2) | -2.50 | 3.10 |
| 2 | CID681 | Asn87(OD1)-N(2) | -0.57 | 3.49 |
| | | Gln71(OE1)-N(2) | -1.61 | 3.28 |
| | | Tyr72(O)-N(2) | -2.50 | 2.96 |
| | | Tyr341(OH)-O(0) | -2.50 | 2.88 |
| | | Asp74(OD2)-O(0) | -2.20 | 3.16 |
| | | Asp74(OD2)-O(1) | -1.40 | 3.32 |
| | | Tyr341(OH)-O(1) | -0.55 | 2.37 |
| 3 | CID439260 | Thr83(OG1)-O(1) | -2.50 | 2.90 |
| | | Ser125(OG)-O(2) | -2.00 | 3.21 |
| | | Trp86(O)-O(2) | -1.10 | 3.38 |
| | | Gly120(O)-O(1) | -1.75 | 3.25 |
| | | Tyr133(OH)-O(1) | -2.20 | 2.56 |
| | | His447(NE2)-N(3) | -2.50 | 2.65 |
| | | Glu202(OE2)-N(3) | -0.14 | 3.27 |
| 4 | CID31211 | Glu202(OE1)-N(3) | -2.50 | 3.10 |
| | | Tyr337(OH)-O(0) | -2.50 | 2.78 |
| | | His447(O)-O(1) | -1.37 | 2.46 |
| 5 | CID65084 | Thr83(OG1)-O(6) | -2.50 | 2.97 |
| | | Thr83(O)-O(6) | -0.36 | 3.46 |
| | | Trp86(O)-O(1) | -0.24 | 3.32 |
| | | Glu202(OE1)-O(2) | -2.50 | 3.10 |
| | | Ser303(OG1)-O(3) | -1.68 | 3.26 |
| | | His447(NE2)-O(3) | -2.50 | 2.60 |
| 6 | CID6047 | His447(NE2)-N(4) | -2.50 | 3.10 |
| | | Glu202(OE2)-N(4) | -2.50 | 2.60 |
| | | His447(O)-O(1) | -2.50 | 2.73 |
| | | Ser125(OG)-O(2) | -1.31 | 2.46 |
| | | Gly120(O)-O(0) | -0.90 | 2.89 |

SN, serial number.

MD simulation. MD simulations were performed using the GROMACS 5.0 (Royal Institute of Technology, Stockholm, Sweden; and Uppsala University, Uppsala, Sweden) installed in Ubuntu Linux 14.0 LTS Intel i5 processor with the standard GROMOS96 43a1 force field (25). MD simulation was performed for the docked protein-ligand complexes and AChE (PDB ID: 4PQE). For the protein and the protein-ligand docked complexes, initially, the system was immersed in a cubic water box and the energy of the complexes was minimized using the steepest descent approach. Following energy minimization, the systems were equilibrated for 100 ps with NVT (number of particles, volume and temperature; canonical) and NPT (number of particles, temperature and pressure; isothermal-isobaric)

ensemble equilibration protocol for ~5,000 steps. Finally, the equilibrated systems were run for 20 ns of MD simulation production under a constant number of particles at 310 K and 1 bar pressure. The trajectory was analyzed and a graph was plotted for the root mean square deviation (RMSD) backbone of AChE and the AChE-ligand complexes.

Results

The AChE inhibitory activities of the plant extracts are presented in Table I. Total alkaloidal extracts from *Nelumbo nucifera*, *Uncaria rhynchophylla* and *Portulaca oleracea* exhibited 76.5, 78.4 and 74.2% inhibition against AChE, respectively (Table I).

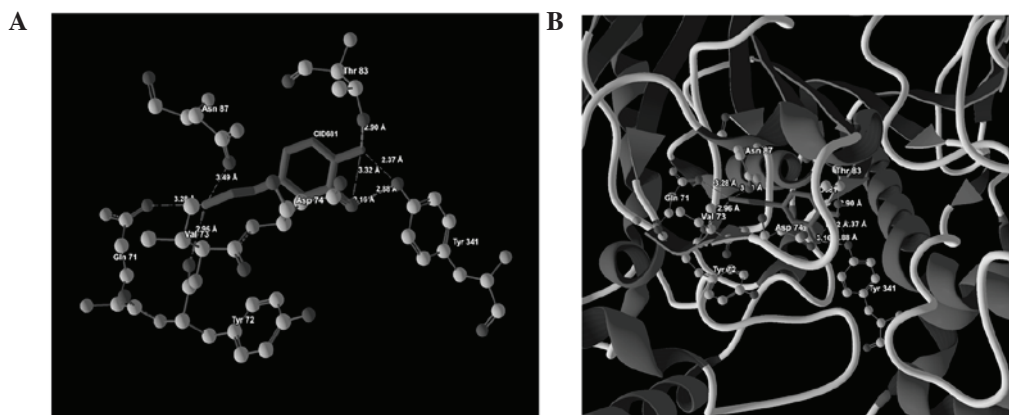


Figure 2. (A) Binding mode of CID681 at the active site region of AChE. (B) Secondary structure depicting the strong molecular interactions formed between CID681 and Tyr71, Gln71, Asp74, Thr83, Asn87, Tyr341 residues of AChE. AChE, acetylcholinesterase.

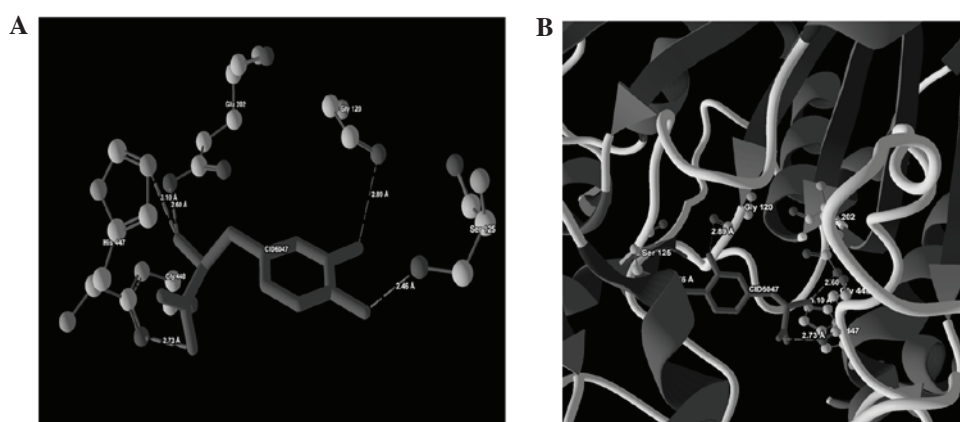


Figure 3. (A) Binding mode of CID6047 at the active site region of AChE. (B) Secondary structure depicting the strong molecular interactions formed between CID6047 and Trp86, Gly120, Ser125, Tyr133, Glu202, His447 residues of AChE. AChE, acetylcholinesterase.

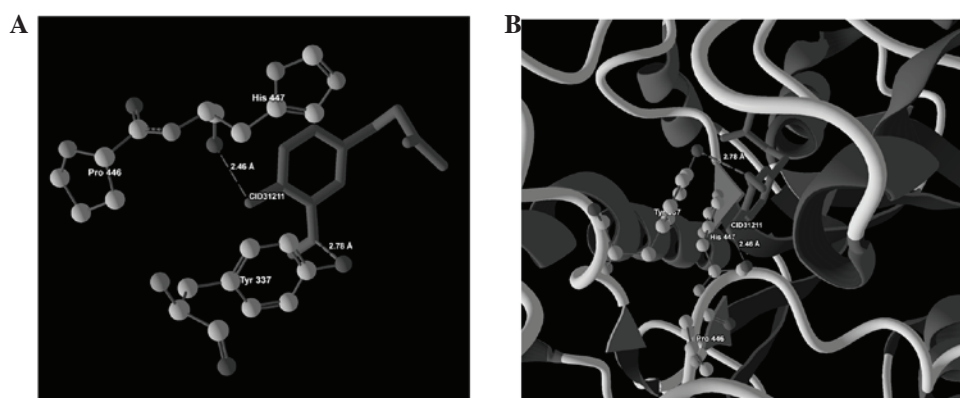


Figure 4. (A) Binding mode of CID31211 at the active site region of AChE. (B) Secondary structure depicting the strong molecular interactions formed between CID31211 and Tyr337, His447 residues of AChE. AChE, acetylcholinesterase.

The compounds present in the herbal plants were retrieved from the NCBI PubChem database, and are presented in Table II. The molecular docking scores of the bioactive compounds present in the herbal plants against AChE are shown in Table III. The scores and results were based on the Rerank and MolDock scores, and interaction energy (24). Rerank Score, MolDock Score and Interaction Energy are measured based on the energy parameters E_{inter} (steric, van der Waals, hydrogen bonding

and electrostatic) between the ligand and the protein, and E_{intra} (torsion, SP2, hydrogen bonding, van der Waals and electrostatic) (24). These energy terms are generated by the MolDock SE algorithm and based on the most stable E_{inter} and E_{intra} ; the compounds were ranked accordingly. The results of the ligand-protein interaction analyses of the top docked compounds against AChE (PDB ID: 4PQE) are presented in Table IV. Images depicting the molecular interactions for the

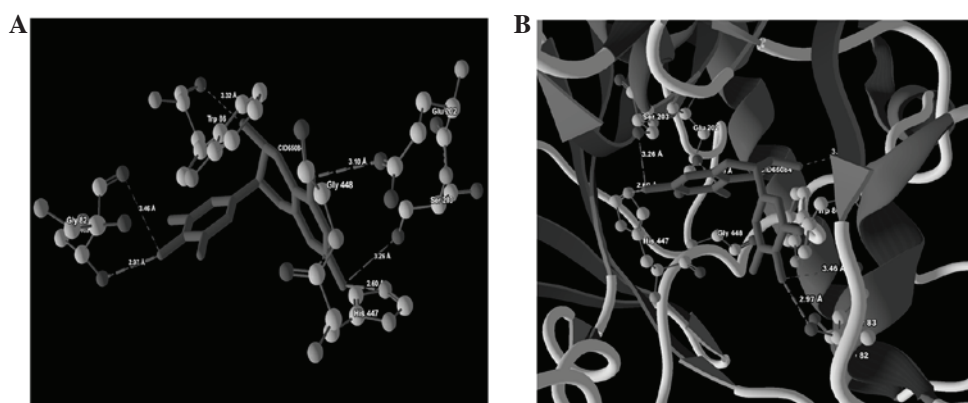


Figure 5. (A) Binding mode of CID65084 at the active site region of AChE. (B) Secondary structure depicting the strong molecular interactions formed between CID65084 and Thr83, Trp86, Glu202, Ser303, His447 residues of AChE. AChE, acetylcholinesterase.

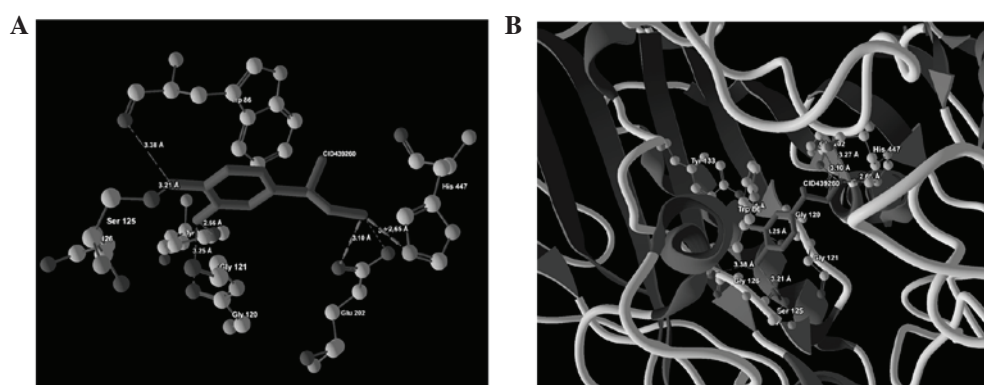


Figure 6. (A) Binding mode of CID439260 at the active site region of AChE enzyme. (B) Secondary structure depicting the strong molecular interactions formed between CID439260 and Gly120, Ser125, Glu202, His447 residues of AChE. AChE, acetylcholinesterase.

top docking hits are presented in Figs. 1-6, and the MD simulation investigating stability of the RMSD backbones of PDB ID: 4PQE and protein-ligand complexes is demonstrated in Fig. 7.

Discussion

In the present study, AChE inhibitory assay of the plant extracts demonstrated that the total alkaloidal extracts from *Uncaria rhynchophylla* (78.4%), *Nelumbo nucifera* (76.5%) and *Portulaca oleracea* (74.2%) exhibited AChE inhibition (Table I). In addition, the alkaloidal extract from *Areca catechu* demonstrated the poorest AChE inhibition (19.3%; Table I).

Molecular docking analysis of the bioactive compounds present in the herbal plants confirmed that certain compounds in *Portulaca oleracea*, *Zingiber officinale* and *Camellia sinensis* possessed strong molecular interactions at the potential ligand binding site of AChE. The major interactions, including bonded and non-bonded interactions, were formed between the docked compounds and the binding cavity of the enzyme. The strength of the ligand-protein interaction was measured by the Rerank score. The Rerank score is a linear combination of E-inter (steric, Van der Waals, hydrogen bonding, electrostatic) between the ligand and the protein, and E-intra (torsion, sp²-sp², hydrogen bonding, Van der Waals, electrostatic) of the ligand weighted by

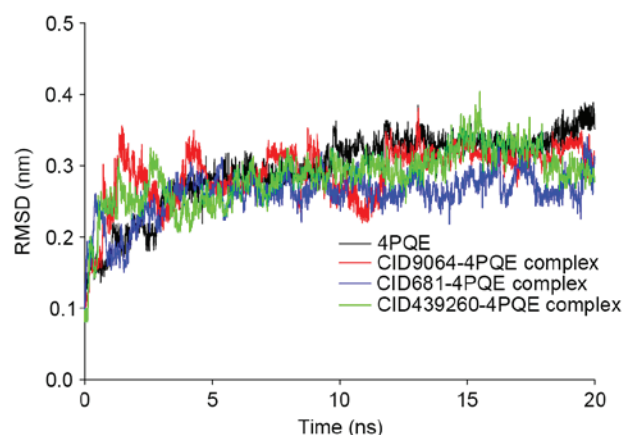


Figure 7. Root mean square deviation (RMSD) backbone of AChE (4PQE), and CID9064-4PQE, CID681-4PQE and CID439260-4PQE complexes.

pre-defined coefficients (24). The Rerank score of the docked compounds along with their MolDock score and interaction energy are shown in Table III. In the present molecular docking simulation analysis, CID9064 (*Uncaria rhynchophylla*) CID681 (*Portulaca oleracea*), and CID439260 (*Portulaca oleracea*) and CID6047 (*Portulaca oleracea*) docked at the binding cavity having a Rerank score of -67.43, -64.76 and -60.40 kJmol⁻¹, respectively. *Uncaria rhynchophylla* and *Portulaca oleracea* exhibited 78.4 and 74.2% AChE

inhibition, respectively. CID 31211 (*Zingiber officinale*) demonstrated a Rerank score of -59.39 and exhibited 60.5% AChE inhibition. Finally, CID65084 (*Camellia sinensis*) had a Rerank score of -53.40 and exhibited 40.2% AChE inhibition.

To understand the in-depth molecular interaction of these compounds with AChE, and its binding mechanism, a ligand-protein interaction analysis for the top 6 docking hits was conducted using a ligand energy inspector. The ligand-protein interaction, including the residues present, their interaction distances and energy, and the interacting atoms of the protein and ligand are presented in Table IV. The molecular docking simulation indicated that the top docking poses were demonstrated to be docked into the binding cavity displaying bonded and non-bonded interactions. Images depicting ligand-protein binding are shown in Fig. 1 (CID9064), Fig. 2 (CID681), Fig. 3 (CID6047) and Fig. 4 (CID31211), Fig. 5 (CID65084) and Fig. 6 (CID439260). The backbone RMSD values of the protein and protein-ligand complexes during 20 ns of MD simulation are presented in Fig. 7, and indicated that the RMSD values for AChE-ligand complexes were more stable suggesting a conformational flexibility and stability in dynamic behavior. Numerous herbal compounds have been demonstrated to have anti-cancer, anti-microbial and anti-inflammatory potential. However, this is not in case of AChE inhibition. In fact, there are few reports on the investigation of herbal compounds as inhibitors of AChE inhibition (26).

In conclusion, *Uncaria rhynchophylla*, *Nelumbo nucifera* and *Portulaca oleracea* possessed strong AChE inhibition. In addition, the molecular docking simulation analyses demonstrated that the active compounds present in *Uncaria rhynchophylla* (CID9061) and *Portulaca oleracea* (CID681 and CID439260) had strong molecular interactions, as evidenced by the molecular docking scores and ligand-protein interaction energy analyses. Furthermore, the MD simulation confirmed the stability of the protein-ligand docked complexes. The results of the present study suggested that CID9064 (catechin), CID681 (dopamine) and CID439260 (norepinephrine) may be key bioactive ingredients that may be prescribed to patients with AD.

Acknowledgements

The authors would like to acknowledge the 5th People's Hospital of Wuhan (Wuhan, Hubei, P.R. China) for necessary support.

References

- Burns A and Iliffe S: Alzheimer's disease. *BMJ* 338: b158, 2009.
- Querfurth HW and LaFerla FM: Alzheimer's disease. *New Eng J Med* 362: 329-344, 2010.
- Todd S, Barr S, Roberts M and Passmore AP: Survival in dementia and predictors of mortality: A review. *Int J Geriatr Psychiatry* 28: 1109-1124, 2013.
- Ballard C, Gauthier S, Corbett A, Brayne C, Aarsland D and Jones E: Alzheimer's disease. *Lancet* 377: 1019-1031, 2011.
- Thompson CA, Spilsbury K, Hall J, Birks Y, Barnes C and Adamson J: Systematic review of information and support interventions for caregivers of people with dementia. *BMC Geriatr* 7: 18, 2007.
- Forbes D, Thiessen EJ, Blake CM, Forbes SC and Forbes S: Exercise programs for people with dementia. *Cochrane Database Syst Rev* 12: CD006489, 2013.
- Mendez MF: Early-onset Alzheimer's disease: Nonamnesic subtypes and type 2 AD. *Arch Med Res* 43: 677-685, 2012.
- Lozano R, Naghavi M, Foreman K, Lim S, Shibuya K, Aboyans V, Abraham J, Adair T, Aggarwal R, Ahn SY, *et al*: Global and regional mortality from 235 causes of death for 20 age groups in 1990 and 2010: A systematic analysis for the Global Burden of Disease Study 2010. *Lancet* 380: 2095-2128, 2012.
- Berchtold NC and Cotman CW: Evolution in the conceptualization of dementia and Alzheimer's disease: Greco-Roman period to the 1960s. *Neurobiol Aging* 19: 173-189, 1998.
- Bonin-Guillaume S, Zekry D, Giacobini E, Gold G and Michel JP: The economical impact of dementia. *Presse Med* 34: 35-41, 2005 (In French).
- Meek PD, McKeithan K and Schumock GT: Economic considerations in Alzheimer's disease. *Pharmacotherapy* 18: 68-73; discussion 79-82, 1998.
- Francis PT, Palmer AM, Snape M and Wilcock GK: The cholinergic hypothesis of Alzheimer's disease: A review of progress. *J Neuro Neurosurg Psychiatry* 66: 137-147, 1999.
- Houghton PJ, Ren YH and Howes MJ: Acetylcholinesterase inhibitors from plants and fungi. *Nat Prod Rep* 23: 181-199, 2006.
- Hardy J and Allsop D: Amyloid deposition as the central event in the aetiology of Alzheimer's disease. *Trends Pharmacol Sci* 12: 383-388, 1991.
- Mudher A and Lovestone S: Alzheimer's disease-do tauists and baptists finally shake hands? *Trends Neurosci* 25: 22-26, 2002.
- Quinn DM: Acetylcholinesterase: Enzyme structure, reaction dynamics, and virtual transition states. *Chem Rev* 87: 955-979, 1987.
- Taylor P and Radić Z: The cholinesterases: From genes to proteins. *Ann Rev Pharmacol Toxicol* 34: 281-320, 1994.
- Sussman JL, Harel M, Frolow F, Oefner C, Goldman A, Toker L and Silman I: Atomic structure of acetylcholinesterase from *Torpedo californica*: A prototypic acetylcholine-binding protein. *Science* 253: 872-879, 1991.
- Radić Z, Gibney G, Kawamoto S, MacPhee-Quigley K, Bongiorno C and Taylor P: Expression of recombinant acetylcholinesterase in a baculovirus system: Kinetic properties of glutamate 199 mutants. *Biochemistry* 31: 9760-9767, 1992.
- Whittaker VP: The contribution of drugs and toxins to understanding of cholinergic function. *Trends Pharmacol Sci* 11: 8-13, 1990.
- Purves D, Augustine GJ, Fitzpatrick D, Hall WC, LaMantia AS, McNamara JO and White LE (eds): *Neuroscience*. 4th edition. Sinauer Associates, Sunderland, MA, pp121-122, 2008.
- Pohanka M: Alpha7 nicotinic acetylcholine receptor is a target in pharmacology and toxicology. *Inter J Mol Sci* 13: 2219-2238, 2012.
- Ellman GL, Courtney KD, Andres V Jr and Feather-Stone RM: A new and rapid colorimetric determination of acetylcholinesterase activity. *Biochem Pharmacol* 7: 88-95, 1961.
- Thomsen R and Christensen MH: MolDock: A new technique for high-accuracy molecular docking. *J Med Chem* 49: 3315-3321, 2006.
- Van Der Spoel D, Lindahl E, Hess B, Groenhof G, Mark AE and Berendsen HJ: GROMACS: Fast, flexible, and free. *J Comput Chem* 26: 1701-1718, 2005.
- Lin HQ, Ho MT, Lau LS, Wong KK, Shaw PC, Wan DC: Anti-acetylcholinesterase activities of traditional Chinese medicine for treating Alzheimer's disease. *Chem Biol Interact* 175: 352-354, 2008.